Mechanism governing surface stress generation

by

Nazita Taghavi

A thesis submitted to the graduate faculty

in partial fulfillment of the requirements for the degree of

MASTER OF SCIENCE

Major: Mechanical Engineering

Program of Study Committee:
Pranav Shrotriya, Major Professor
Ganesh Balasubramanian
Ashraf Bastawros

Iowa State University

Ames, Iowa

2014

DEDICATION

This thesis is dedicated to my parents for their endless love and sacrifices.

TABLE OF CONTENTS

ABSTRACT

Microcantilever based sensors can be used for detection of specific target molecules in a solution. In conventional mode of sensing, receptor molecules are immobilized on the cantilever surface and the chemical interaction between receptors and ligand molecules causes surface stress change resulting in cantilever deformation; however, in the competition mode of sensing, the cantilever surface is covered with complex molecules and after immerging cantilever in the solution of target molecules, ligand molecules diffuse away from the cantilever surface and causes cantilever deflection. In this method, the rate of ligand dissociation can be measured as a sensing tool.

In this report, both mode of sensing is considered and theoretical models are developed to understand the mechanism of cantilever tip deflection in conventional mode of sensing and ligand dissociation rate in competition mode of sensing.

For the conventional mode of sensing, it is shown that, the molecular interaction model, which is based on interaction energy between double strand DNAs, can predict the cantilever deflection better than entropy model.

Also, it is proved that the competition mode of sensing can be a good method of sensing and its advantages and limitations are shown.

CHAPTER I

INTRODUCTION

1.1 Introduction to micro-cantilever biosensors

In last fifteen years, microcantilever sensors have been emerging for the detection of chemicals and biological substances [1-7]. A cantilever biosensor consists of a layer of biomolecules that can bind with target molecules in the solution, cause surface stress change and consequently mechanical deformation of the microcantilever. The cantilever deflection can be measured and used as a tool for detection of specific molecules [8].

Detection of biomolecules by using cantilever biosensors has become significant in variety areas like medical diagnostics because of small size, lightweight, and high sensitivity of these biosensors [3, 8]. Many experimental and theoretical studies have been conducted to investigate the sensing mechanism. Fritz et al. [9] performed hybridization experiments with single stranded DNA (ssDNA) of 12 nucleotides and different concentration values of complementary strands in hybridization buffer. The cantilever array was immersed in liquid cell and cantilever deflection was measured by an optical beam deflection technique. It was shown that the cantilever nano-mechanical responses can be measured for not only recognition of complementary DNA strands in the solution, but also discrimination of DNA strands with single base-pair mismatch. Followed Fritz et al. Hansen et al. [10] also conducted experiments with 20 and 25-nt probe DNAs and 10-nt target strands with one or two internal mismatches and showed that the cantilever based biosensors can detect DNAs with different number and position of mismatches.

To understand the mechanism of transducing chemical energy to mechanical work in such biosensors, Stachowiak et al. [11] performed experiments with DNAs with three different molecular lengths. He also used different salt concentration in buffer during immobilization and hybridization to control the immobilization density and hybridization efficiency. Results of his experiments showed that although the immobilization density, hybridization efficiency and the molecule length affect cantilever deflection, the effects of all three parameters can be coupled and surface stress produced by DNA hybridization can be directly related to hybridization density or surface coverage.

To predict cantilever deflection, Hagan et al. [12] proposed a mathematical model in which he assumed hexagonal arrangement for immobilized ssDNAs and considered hydration and electrostatic forces as well as conformational entropy. Based on his model, he concluded that hydration forces dominantly influence the cantilever deformation during hybridization. Begley et al. [13] also proposed another model based on the thermodynamics of adsorption and interaction energy between adsorbed molecules on the surface of biosensor array. He showed that the change in surface stress can be expressed by pair interaction potential and pair correlation function and considered three different boundary conditions (cantilevered, pinned and clamped boundary conditions) for sensing films to calculate the deformation of the sensor array. The equation explained surface stress change based on pair potential and correlation function was based on Virial theorem. Unfortunately, there are some mistakes in driving this equation. Later in this report, that equation will be modified.

Huang et al. [14] suggested that the orientational entropy of dsDNAs are changed after the molecule is absorbed to the sensor film because the neighboring molecules occupy the space needed for freely rotation of molecule and eliminate a fraction of possible

configurations of the molecule. Considering hexagonal arrangement for immobilized ssDNAs and hundred percentage for hybridization efficiency, he proposed interaction potential between dsDNAs based on entropy change and using the same idea of calculating surface stress change by pair interaction potential and pair correlation function, he predicted the deformation of circular membrane as sensing film. His model had some limitation. First, the pair interaction potential could be considered for just neighboring molecules and interaction of molecule with other molecules was eliminated. Also, the Monte Carlo simulation showed that this model could be used for very small molecular separations where the ratio of separation and effective molecular diameter was less than 2. The model suggested an effective molecular diameter based on salt concentration and molecular bending that made no sense. The Author also asserted other interaction potentials like the one proposed by Stery et al. [15, 16] could capture the same trend as the mentioned pair potential that was a wrong claim. In addition, that model could not capture the effect of hybridization efficiency.

Zhao et al. [17] suggested a mathematical and numerical model based on Strey interaction potential. He assumed four different DNA ensembles: average spacing, random selection, energy minimization, and Gaussian-perturbed and instead of directly calculating surface stress change by the concepts of pair potential and correlation function, the energy of molecular samples were calculated numerically and the total energy of the system including interaction energies and bending energy were minimized to determine the cantilever tip deflection. While the advantages of random selection and energy minimization ensembles over average spacing samples were that they could present the effects of different hybridization efficiencies, Gaussian-perturbed samples could capture the effect of molecular disorders as well. Based on numerical calculations, average spacing, random selection,

energy minimization ensembles could predict experimental results for high immobilization densities equal or over 0.13 nm^{-2}, but for lower densities between 0.01 to 0.1 nm^{-2}, reasonable results could be given by Gaussian-perturbed ensembles.

In all mathematical and experimental studies mentioned above, the same mechanism for the sensing was assumed: the cantilever surface was covered with receptor species that could combine with ligand molecules in the solution and cause cantilever bending. Kang et al. [18] called this sensing method as conventional or direct mode of sensing and found some limitation in sensing with this method especially when the concentration of ligand molecules in the solution were so low. He proposed an alternative method of sensing called competition mode of sensing. In this method, the surface of the cantilever is covered with ligand-receptor complexes and the cantilever is immersed in the solution of receptors. Because of the competition between surface receptors and soluble receptors to react with ligand molecules, the ligand molecules diffuse away from the cantilever that causes cantilever deflection.

In this report, both conventional and competition mode of sensing is considered. First, equations for calculation of surface stress change based on pair potential and change of entropy is modified and then based on entropy change, a model for prediction of cantilever deflection is expressed. In this model, the effect of attraction forces between molecules and gold surface of cantilever is taken to account. Then, a mathematical model for explaining the mechanism of competition sensing mode is reported.

1.2 Molecular arrangements

As mentioned above, for detection of special molecules in a solution, surface of micro-cantilever bio-sensor is covered by single strand DNAs (ssDNAs) with certain

immobilization density. After immersing cantilever in the solution of target molecules, the complementary parts can hybridize with a certain percentage of these ssDNAs and form hybridized double strand DNAs (dsDNAs). In our model, we assume the arrangement of ssDNAs having been immobilized on the surface of cantilever is hexagonal and the complementary parts hybridize with them based on hybridization efficiency.

For the numerical studies, two configurations of molecules are considered (Figure 1.1). SsDNAs (light blue circles in Figure 1.1) are flexible molecules that can rotate around themselves; however, dsDNAs (dark blue rods) can be assumed as stiff cylindrical rods since the length of dsDNAs in our model is maximum 30 nucleotides and can be considered short DNAs in comparison with persistence length of dsDNA. In the stand-up configuration, dsDNA are assumed to be vertical to the surface of the micro-cantilever and parallel to each other. In lie-down configuration, the molecules lie on the surface of the cantilever due attraction forces between molecules and the layer of gold on the surface of cantilever. In this configuration, dsDNAs tend to have the same directions to minimize the energy interaction between molecules.

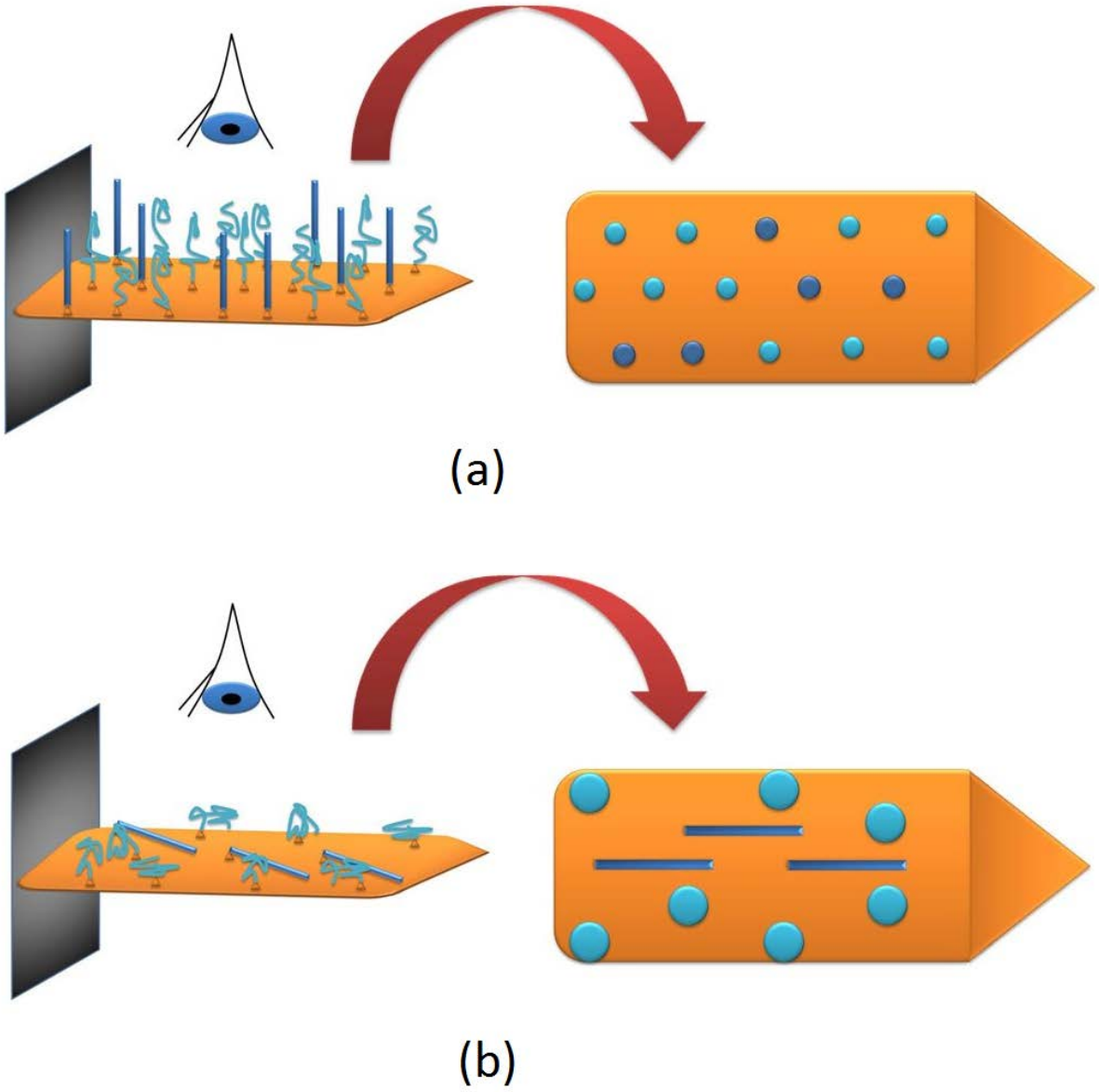

Figure 1.1. *Two configuration of molecules: (a) stand-up and (b) lie-down configuration*

CHAPTER II

CONVENTIONAL MODE OF SENSING

2.1 Molecular interaction model

The molecular interaction model is based on interaction forces between dsDNAs. Since the interaction forces between dsDNAs are much stronger than ssDNAs, the interaction energy after hybridization causes cantilever deflection. To find the cantilever tip deflection, Virial theorem can be used. Virial theorem is based on energy conservation theory and can be written as follow [19]:

$$\langle \mathcal{W}^{tot} \rangle = \langle \mathcal{W}^{int} \rangle + \langle \mathcal{W}^{int} \rangle, \tag{2.1}$$

where $\langle \mathcal{W}^{tot} \rangle$ is the total virial, $\langle \mathcal{W}^{int} \rangle$ is the internal virial and $\langle \mathcal{W}^{ext} \rangle$ is the external virial. The total virial over N molecules is

$$\langle \mathcal{W}^{tot} \rangle = \frac{1}{2} \langle \sum_{i=1}^{N} r_i . f_i^{tot} \rangle = -N K_B T, \tag{2.2}$$

where K_B is Boltzmann constant and T is temperature. The symbol f_i^{tot} shows the sum of intermolecular and external forces. The internal virial and the external virial are

$$\langle \mathcal{W}^{int} \rangle = \frac{1}{2} \langle \sum_{i=1}^{N} r_i . f_i^{int} \rangle, \tag{2.3}$$

$$\langle \mathcal{W}^{ext} \rangle = \frac{1}{2} \langle \sum_{i=1}^{N} r_i . f_i^{ext} \rangle = -\gamma_0 A, \tag{2.4}$$

where the γ_0 is surface stress and A is the surface of the cantilever. The internal virial can be written as function of pair virial, w, as follow:

$$\langle \mathcal{W}^{int} \rangle = -\frac{1}{2} \langle \sum_i \sum_{j>i} w(r_{ij}) \rangle, \tag{2.5}$$

where r_{ij} is the vector between the molecular centers and

$$w(r_{ij}) = r_{ij}\frac{\partial v(r_{ij})}{\partial r_{ij}}, \tag{2.6}$$

where $v(r_{ij})$ is pair potential and we have

$$\langle \sum_i \sum_{j>i} w(r_{ij}) \rangle = \frac{1}{2} N\rho \int_0^\infty w(r) g(r) (2\pi r) dr, \tag{2.7}$$

where $g(r)$ is the pair distribution function. From equations (2), (4) and (7) we have

$$\gamma_0 = \rho K_B T - \frac{\rho^2 \pi}{2} \int_0^\infty r^2 g(r)\, v'(r) dr. \tag{2.8}$$

Since the molecules are attached to the surface of the cantilever, we can assume the kinetic energy of the molecules are zero and the first term of the left side of the equation (8) can be ignored. For the molecules attached on the cantilever surface, the pair distribution function can be written as follow:

$$g(r) = \sum_{i=1}^{\infty} \frac{N_i}{2\pi r \rho} \delta(r - r_i), \tag{2.9}$$

where δ is Dirac delta function. By substituting equation (9) into equation (8) we have:

$$\gamma_0 = -\frac{\rho}{4} \sum_{i=1}^{\infty} N_i r_i\, v'(r_i). \tag{2.10}$$

The pair interaction potential between dsDNA molecules can be calculated based on Strey et al. [12, 13] model. The Strey pair potential can be written as follow:

$$v(r_i) = v_o(r_i) + cK_B T K_C^{-1/4} L_{DNA} \sqrt[4]{\frac{\partial^2 v_o(r_i)}{\partial r_i^2} - \frac{1}{r_i}\frac{\partial v_o(r_i)}{\partial r_i}}, \tag{2.11}$$

where c is a dimensionless constant, L_{DNA} is the length of DNA, K_C is $K_B T l_p$, l_p is persistence length of dsDNA molecules and $v_o(r_i)$, the summation of energy of electrostatic repulsion and hydration force interactions, is as follow:

$$v_o(r_i) = \vartheta_D \frac{exp(-r_i/r_d)}{\sqrt{r_i/r_d}} + \vartheta_H \frac{exp(-r_i/r_H)}{\sqrt{r_i/r_H}}, \tag{2.12}$$

where ϑ_D and ϑ_H are empirical constants, r_d is Debye screening length and r_H is the correlation length of water.

Figure 2.1 shows the results of molecular interaction model for the three Zhao et al. [17] ensembles, average spacing, random selection and energy minimization, considering stand up configuration. Numerical study of this model having been shown in Figure 2.1, has given us exactly the same results as Zhao's energy minimization model for different immobilization density and hybridization efficiencies; therefore, it can be concluded this model can be a good modification for Begley et al. [13] model and an easier method of calculating the surface stress change in comparison with Zhao's model.

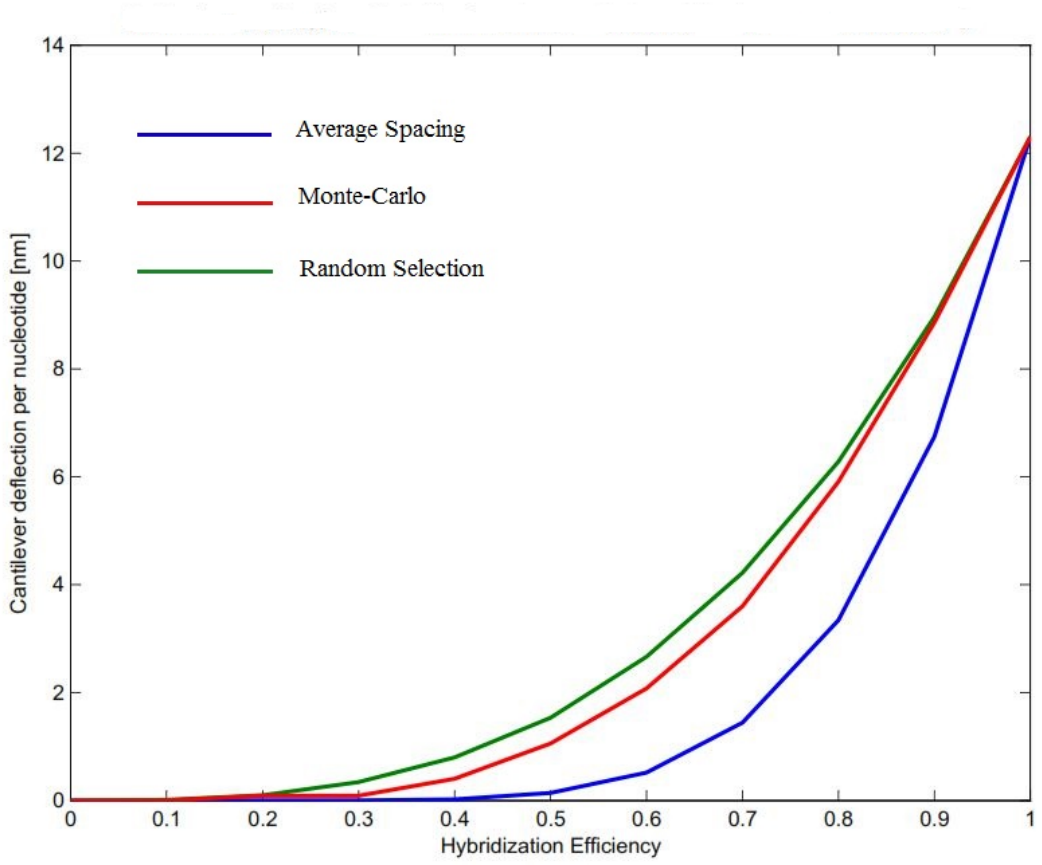

Figure 2.1. *Cantilever deflection as a function of hybridization efficiency for immobilization density at* $0.13\ nm^{-2}$

2.2 Entropy model for stand-up configuration of molecules

In this model, the hexagonal arrangement of ssDNAs (Figure 2.2) and high packing density is considered and the Boltzmann's entropy equation can be used to calculate the change in entropy of molecules after hybridization based on the number of ways that the DNA molecule is mostly arranged. Boltzmann equation can be written as follow:

$$S = K_B \ln(W), \tag{2.13}$$

where W is the number of microstates. From the first law of thermodynamics, we have:

$$\Delta E = N_A T \Delta S, \tag{2.14}$$

where ΔE is the change in energy of all molecules after hybridization that causes surface stress change, $N_A$is the number of molecules (ssDNAs) in smallest sample area, A (Figure 2), and ΔS is the change in entropy of molecules. For hybridization efficiency of 100%, N_A is equal to 1. For hybridization efficiencies lower than 100%, $N_A$is equal to hybridization efficiency.

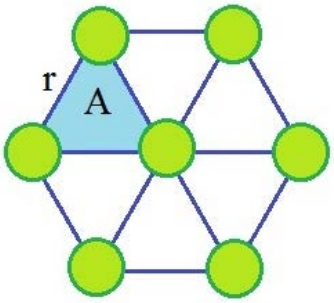

Figure 2.2. *Hexagonal arrangement of molecules*

The surface stress change, γ_0, causes cantilever deflection is

$$\gamma_0 = \frac{\partial \Delta E}{\partial A}, A = \frac{\sqrt{3}}{4} r, \tag{2.15}$$

Huang et al. [14] suggested that for 100% hybridization efficiency, each dsDNA is surrounded by six other dsDNAs and limited its rotation. He assumed the number of microstates for the surrounded DNA could be related to the solid angle accessible to that molecule (Figure 2.3).

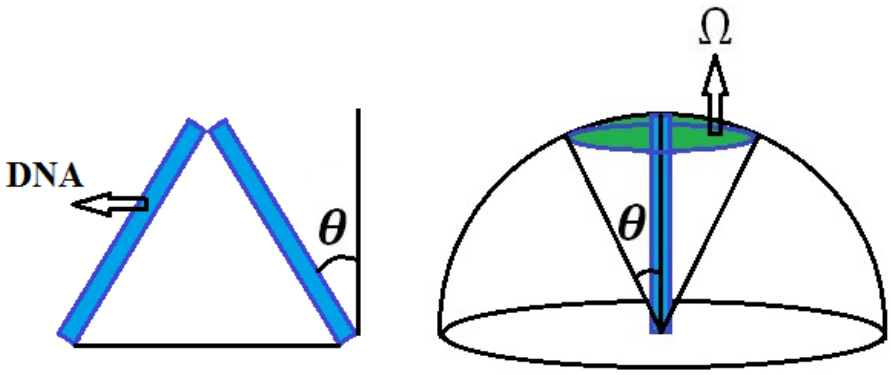

Figure 2.3. *DNA motion and solid angle accessible by DNA*

The solid angle, Ω, can be written as follow:

$$\Omega = \int_0^{\theta} 2\pi \sin\theta \, d\theta = 2\pi \left[1 - \sqrt{1 - \left(\frac{r-d}{2L}\right)^2}\right], \tag{2.16}$$

where d is the diameter of the molecule and L is the length of the molecule. Therefore

$$\Delta E = N_A T K_B \ln\left(\frac{\Omega}{2\pi}\right), \tag{2.17}$$

and

$$\gamma_0 = \frac{2}{\sqrt{3}r} N_A T K_B \frac{\Omega'(r)}{\Omega(r)}. \tag{2.18}$$

For very high packing densities and hybridization efficiencies lower than 100%, still we can assume the molecule rotates in a cone like Figure 2.3 but for very low concentrations, this model may not work. The surface stress change calculated by this equation can be a modification for Huang's model.

2.3 Entropy model for lie-down configuration of molecules

DNA molecules tend to lie on the surface of the cantilever because of the attraction force between gold and DNA molecules. When dsDNA lies, it may be surrounded by other dsDNAs or ssDNAs and those molecules can limit the motion of the molecule and consequently cause surface stress change. If the molecular separation is r, we assume every molecule occupies $\frac{r}{2}$ (Figure 2.4). Also, we assume the free end of dsDNA molecule can be separated from the cantilever surface. The height that the free end of molecule can goes up is considered so small and about few nanometers to model lie-down configuration. Figure 2.5 shows the cross section area of the dsDNAs. a and b are the height of the separation of molecule from cantilever surface and the distance the molecule can rotate respectively. Like for stand-up configuration, the surface area accessible for the free end of dsDNA can be calculated as number of microstates as follow:

$$\varphi = \int_0^a \int_0^{b\sqrt{1-\frac{x^2}{a^2}}} \frac{L}{\sqrt{L^2-x^2-y^2}} dydx. \tag{2.19}$$

The change in energy is

$$\Delta E = N_A T K_B \ln(\frac{\varphi}{4\pi L^2}), \tag{2.20}$$

and

$$\gamma_0 = \frac{2}{\sqrt{3}r} N_A T K_B \frac{\varphi'(r)}{\varphi(r)}. \tag{2.21}$$

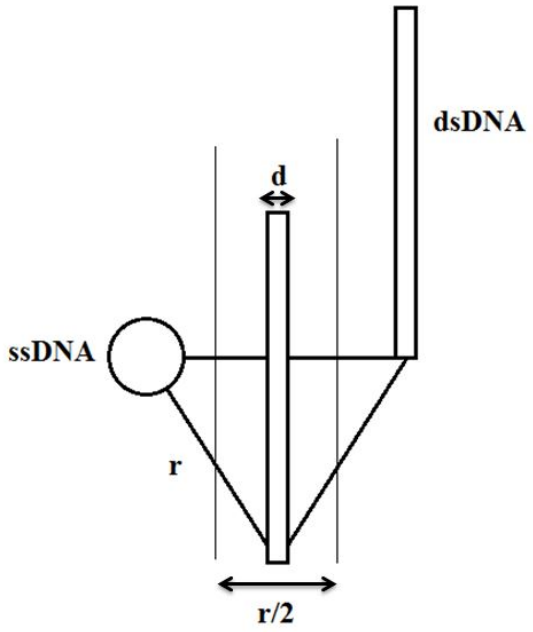

Figure 2.4. *Geometrical modeling of lie-down configuration*

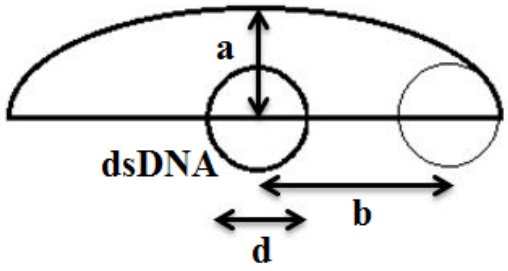

Figure 2.5. *Height of separation and rotational distance*

2.4 Discussion on entropy model for lie-down configuration

In order to find surface stress change for different immobilization densities and hybridization efficiencies, the function φ and its derivative can be calculated numerically. Figure 2.6 shows the change in surface stress as a function of molecular separation when the diameter of the dsDNA is about 2 nm. It can be seen that when the molecular separation is a

value close to twice the dsDNA diameter, the surface stress change can be so high. From Figure 2.7 also the same result can be seen. Figure 2.7 has been plotted for when the molecular separation is 4 nm. When the diameter of the molecule is approximately 2 nm, we get very large results for surface stress value.

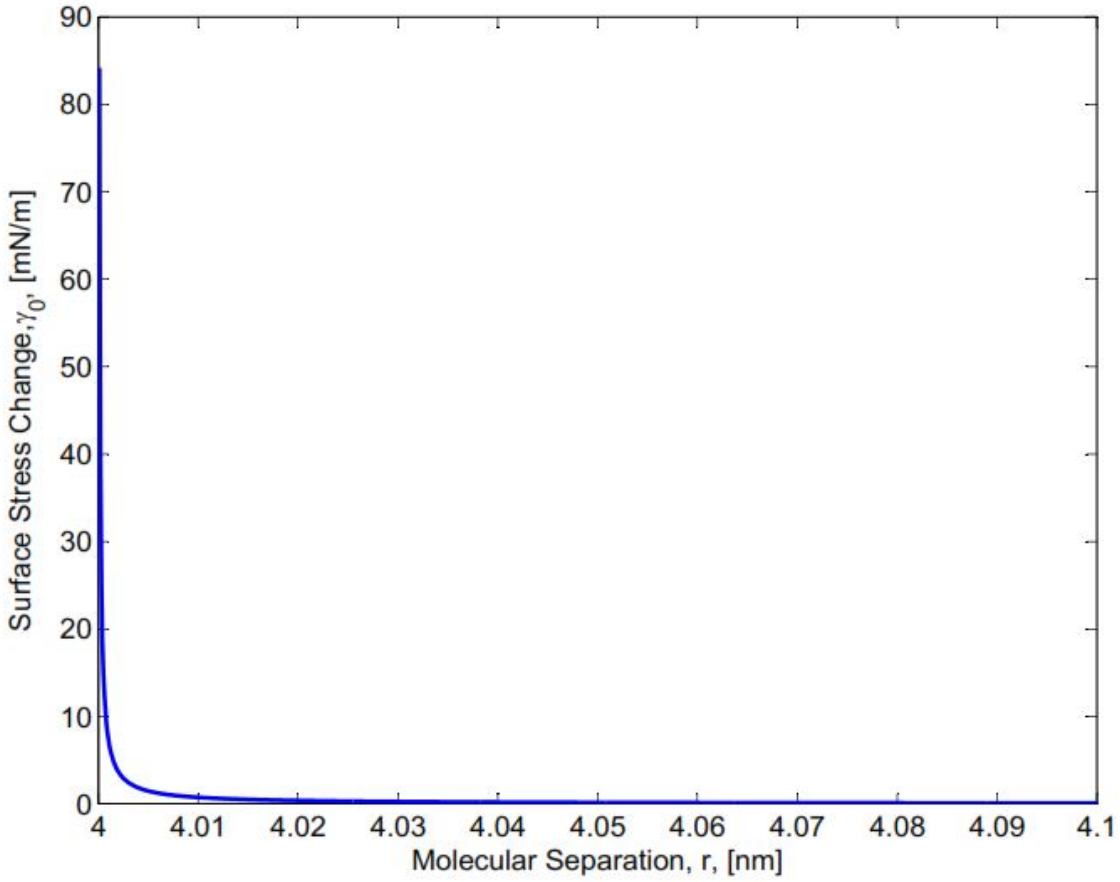

Figure 2.6. *Surface stress change as a function of molecular separation*

Figures 2.6 and 2.7 confirms the Hagan et al. [12] claim that the change in entropy of molecules after hybridization doesn't have the dominant contribution in cantilever deflection when the molecular separation is large in comparison with molecule size, but for small separation, the effect of entropy change should not be ignored. To the best of author knowledge, still there is no explicit equation to show the dependence of effective diameter of

molecule with hybridization buffer salt concentration, but Figure 2.6 and 2.7 show that, the salt concentration of buffer also can be significant for small separation of molecules.

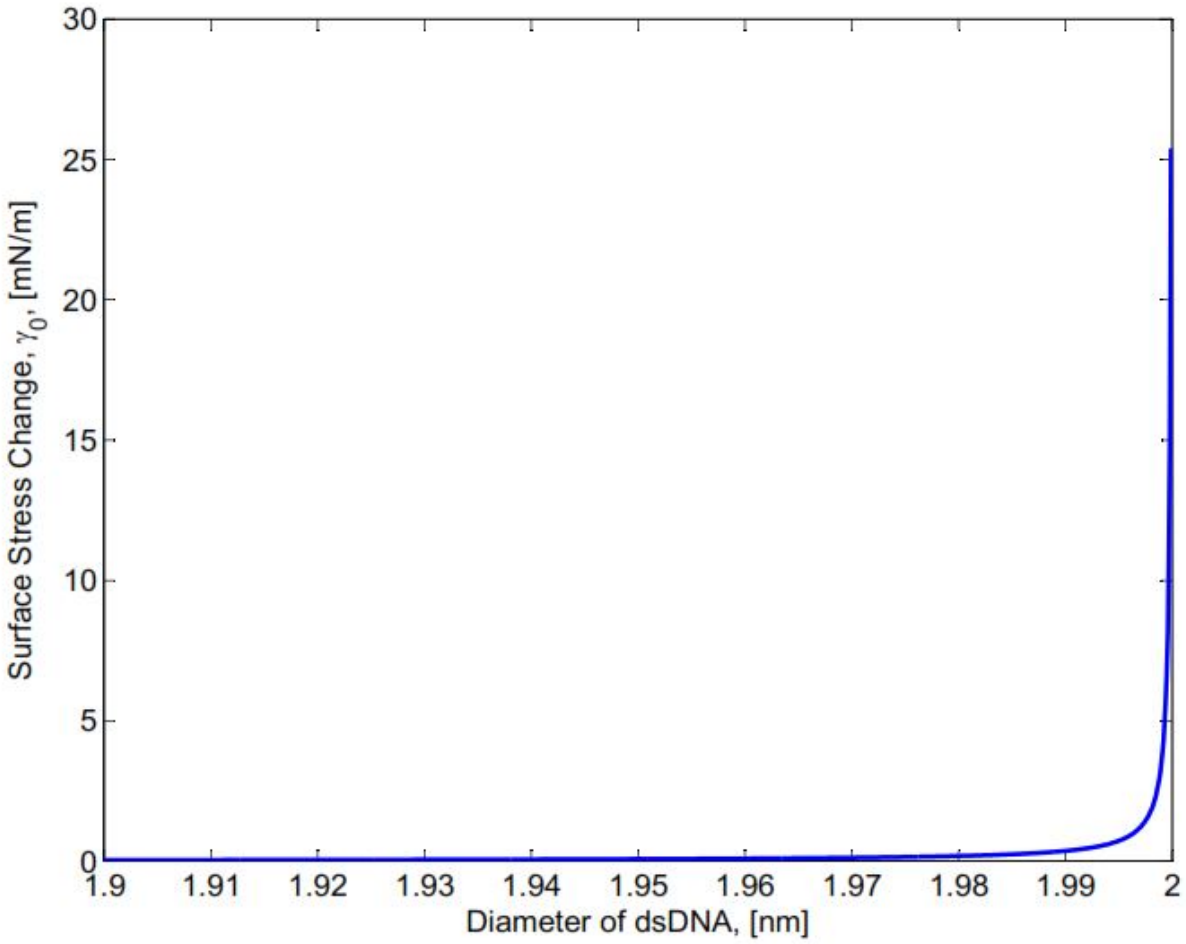

Figure 2.7. *Surface stress change as a function of dsDNA diameter*

Figure 2.8 shows the results of this model in comparison with Stachowiak experimental results [11]. The simulation has done for dsDNA diameter of 2 nm and the molecular separation of approximately 4 nm. We have slightly changed the molecular separation from 4.0001 to 4.0008 and hybridization efficiency from %22 to %45. Authors do not claim that the Stachowiak's experiments have been done exactly at these molecular

separations and hybridization efficiencies. This plot just shows that the results of this model are in the reasonable range when the molecular separation is small with respect to DNA molecule size.

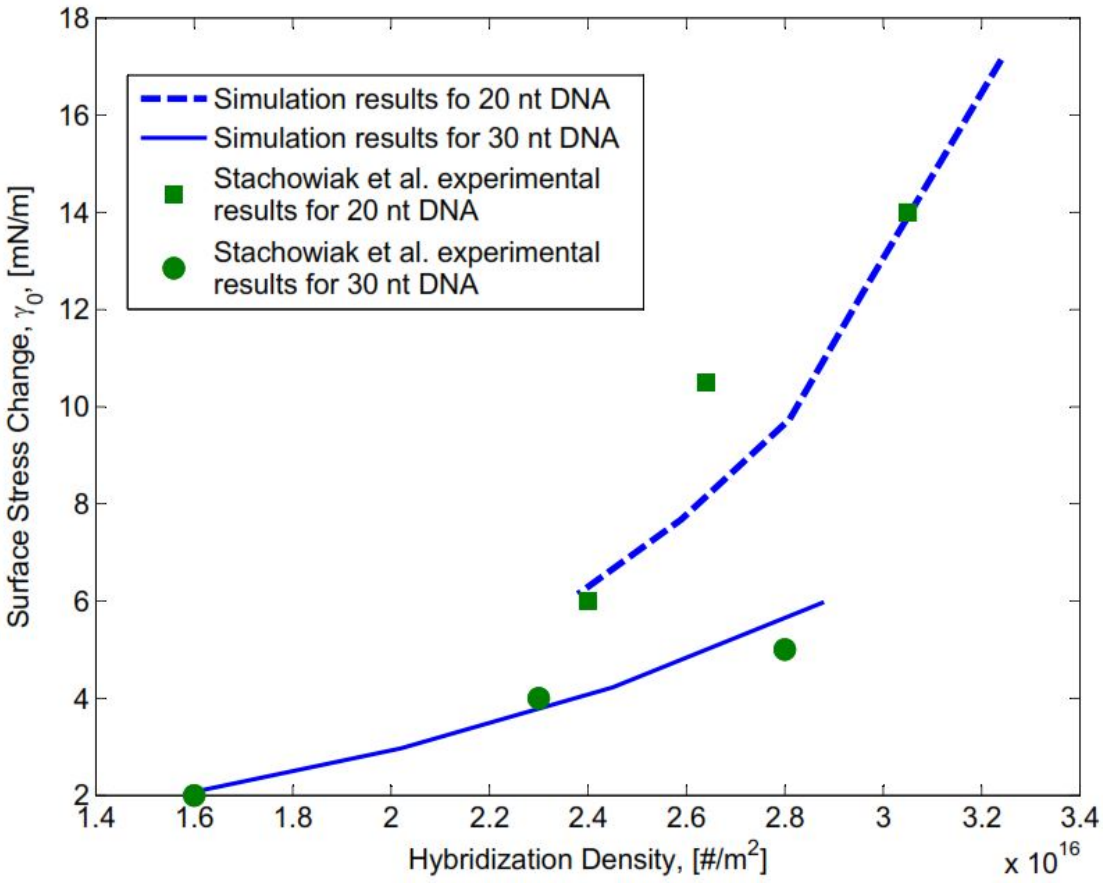

Figure 2.8. *Comparison of simulation results with experimental results*

Since this model is too sensitive to molecular separation and cannot predict the surface stress change when the molecular separation is large, we cannot consider this model as a good model for prediction of cantilever deflection. The only conclusion for this model is that, the change in entropy of the system can be important for some special molecular separation.

CHAPTER III

COMPETITION MODE OF SENSING

3.1 Theoretical model for competition sensing mode

In competition sensing mode, the surface of micro-cantilever biosensor is covered with complex molecules (Figure 3.1 (a)). The concentration of ligands in the solution of receptors is initially zero but after immersing biosensor in the solution of target molecules, ligand molecules are immediately unbound from the cantilever and distributed uniformly within the local layer with thickness of δ (Figure 3.1 (b)). These molecules can bind again with receptors on the surface of cantilever, or reversibly bind with available receptors in the local layer. They are also transported out of the local layer by diffusion.

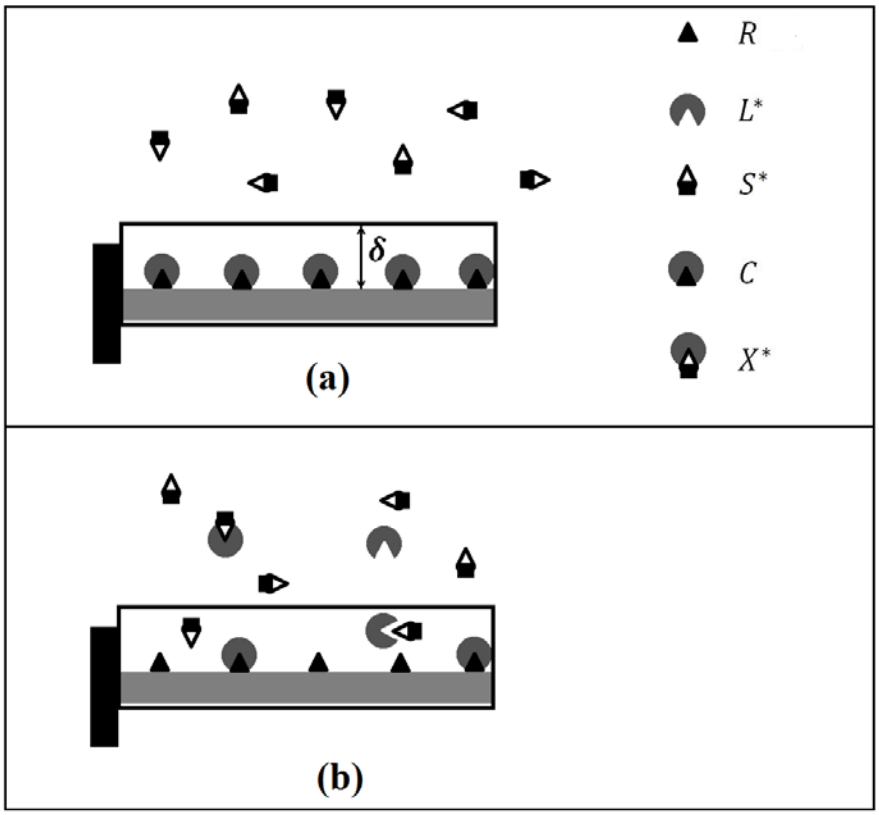

Figure 3.1. *Physical model of competition sensing mode*

Since the micro-cantilever size is so small in comparison with the size of container of solution, we can assume the micro-cantilever is a small particle like a spherical cell with radius a and a reversible binding of ligands, with receptors on the surface of the cell can take place in a local layer (Figure 3.2). The mathematical analysis of competition between receptors on the cell and receptors in the solution for binding with ligands is not a new topic. Kimberly et al. [20, 21] theoretically analyzed the competition of soluble receptors and cell receptors in secretion of ligands in order to inhibit cellular receptor bindings in tumor cells. His model can be modified to develop a new mathematical model which can be used to investigate the completion sensing mode.

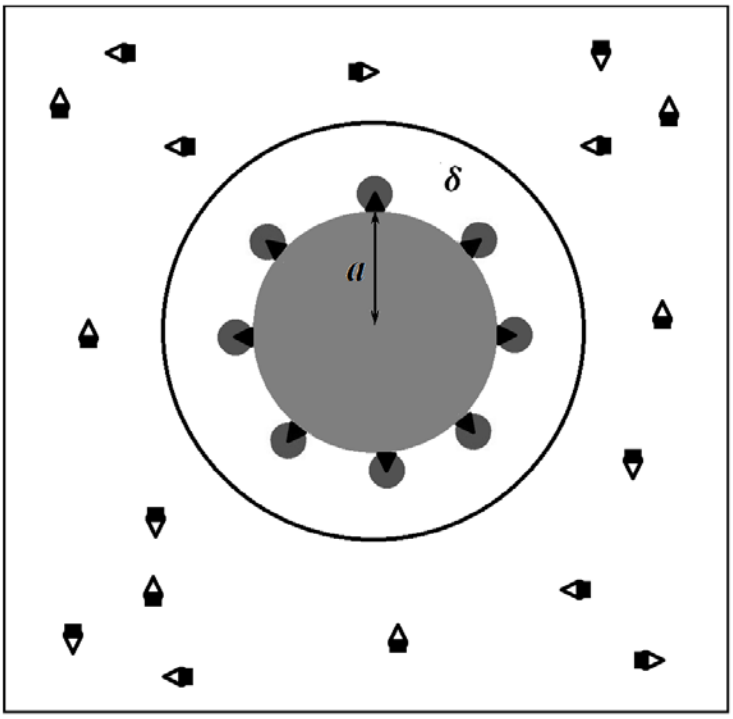

Figure 3.2. *Spherical cell model*

The change of complexes or bound receptors, C and unbound surface receptors, R can be expressed as follow:

$$\frac{dR}{dt} = -k_{on}L^*R + k_{off}C, \tag{3.1}$$

$$\frac{dC}{dt} = k_{on}L^*R - k_{off}C, \tag{3.2}$$

where, k_{on} and k_{off} are on- and off-rates of binding and L^* is concentration of ligand. The kinetic characteristic of transporting ligands between the local layer and surrounding media also can be expressed by the Smoluchowski diffusion-controlled theory [22, 23] for a sphere cell as follow:

$$V^*\frac{dL^*}{dt} = -k_{on}L^*R + k_{off}C - V^*k_{on}^sL^*S^* + V^*k_{off}^sX^* - 4\pi D_L(a+\delta)L^*, \tag{3.3}$$

where V^* is the local volume, S^* is the concentration of soluble receptors, k_{on}^s and k_{off}^s are binding and unbinding rate constants of ligand and soluble receptor, D_L is diffusion coefficient and X^* is the concentration of complexes in the local volume. Ligand molecules out of the local volume may be transported into the layer with a diffusion coefficient D_s and transport to the local layer again can be characterized by the Smoluchowski diffusion-controlled constant to a sphere. Kinetic expressions for the change rates in soluble receptors and complexes within the secretion layer, S^* and X^* are:

$$V^*\frac{dS^*}{dt} = -V^*k_{on}^sL^*S + V^*k_{off}^sX^* + 4\pi D_s(a+\delta)(S_B - S^*), \tag{3.4}$$

$$V^*\frac{dX^*}{dt} = V^*k_{on}^sL^*S - V^*k_{off}^sX^* - 4\pi D_s(a+\delta)(X^*), \tag{3.5}$$

where S_B is the initial concentration of soluble receptors. To investigate the effects of different parameters, it is convenient to nondimensionalize surface coverage with C_0A, concentrations with $\frac{C_0}{\delta}$ and time with $\frac{1}{k_{off}}$ where C_0 is the initial surface density of complexes on the cantilever surface and A is the outer surface of the cell. The nondimensional form of equations (3.1)-(3.6) is:

$$\frac{dR_n}{dt_n} = -A_n L_n^* R_n + C_n, \tag{3.7}$$

$$\frac{dC_n}{dt_n} = A_n L_n^* R_n - C_n, \tag{3.7}$$

$$\frac{dL_n^*}{dt_n} = -A_n L_n^* R_n + C_n - k_n A_n L_n^* S_n^* + K_f X_n^* - D_{Ln} L_n^*, \tag{3.8}$$

$$\frac{dS_n^*}{dt_n} = -k_n A_n L_n^* S_n^* + k_f X_n^* - D_{Sn}(SB_n - S_n^*), \tag{3.9}$$

$$\frac{dX_n^*}{dt_n} = k_n A_n L_n^* S_n^* - k_f X_n^* - D_{Sn} X_n^*, \tag{3.10}$$

where

$$k_n = \frac{k_{on}^S}{k_{on}} \qquad k_f = \frac{k_{off}^S}{k_{off}}$$

$$D_{Ln} = \frac{4\pi D_L(a+\delta)}{A\delta k_{off}} \qquad D_{Sn} = \frac{4\pi D_S(a+\delta)}{A\delta k_{off}} \tag{3.11}$$

$$A_n = \frac{C_0}{\delta k_D} \qquad k_D = \frac{k_{off}}{k_{on}}$$

3.2. Numerical results and discussion

As it stated before, micro-cantilever biosensor with complexes on its surface is immersed in the solution of target molecules. Prediction of the change in number of complexes and receptors on the surface of the cantilever with time, therefore, can be a strong tool for evaluating existence of a special target molecule, its concentration in the solution and cantilever tip deflection. In this section, the effects of different physical parameters on number of complexes and receptors are discussed. In order to apply for specific geometry, the outer surface of the cell, A, for about 10000 μm^2 and local layer thickness, δ, for about 5 μm is used in numerical examples throughout this paper.

Figure 3.3 shows the change of nondimensional number of complexes and receptors on the cantilever surface with time when the ligand molecules are small. Here, the constant rate of

binding, k_{on}, is $3.5 \times 10^2\ M^{-1}s^{-1}$ [24] and the equilibrium constant, k_D, is $20\ \mu M$. The diffusion coefficients for small receptor molecule like cocaine, D_S, is $1.6 \times 10^{-6}\ cm^2/s$ and large ligand like 30 nt DNA aptamer, D_L, is $5.2 \times 10^{-6}\ cm^2/s$. These numbers can be estimated based on the molecular weight of the molecules. The rate constant of the ligand and soluble receptors, k_{on}^s and the equilibrium constant, k_D^s are assumed to be equivalent to k_{on} and k_D respectively. Fig. 2 shows that after the cantilever is put into the solution, ligand DNAs are dissociated into the solution and the rate of dissociation is larger in the first time intervals.

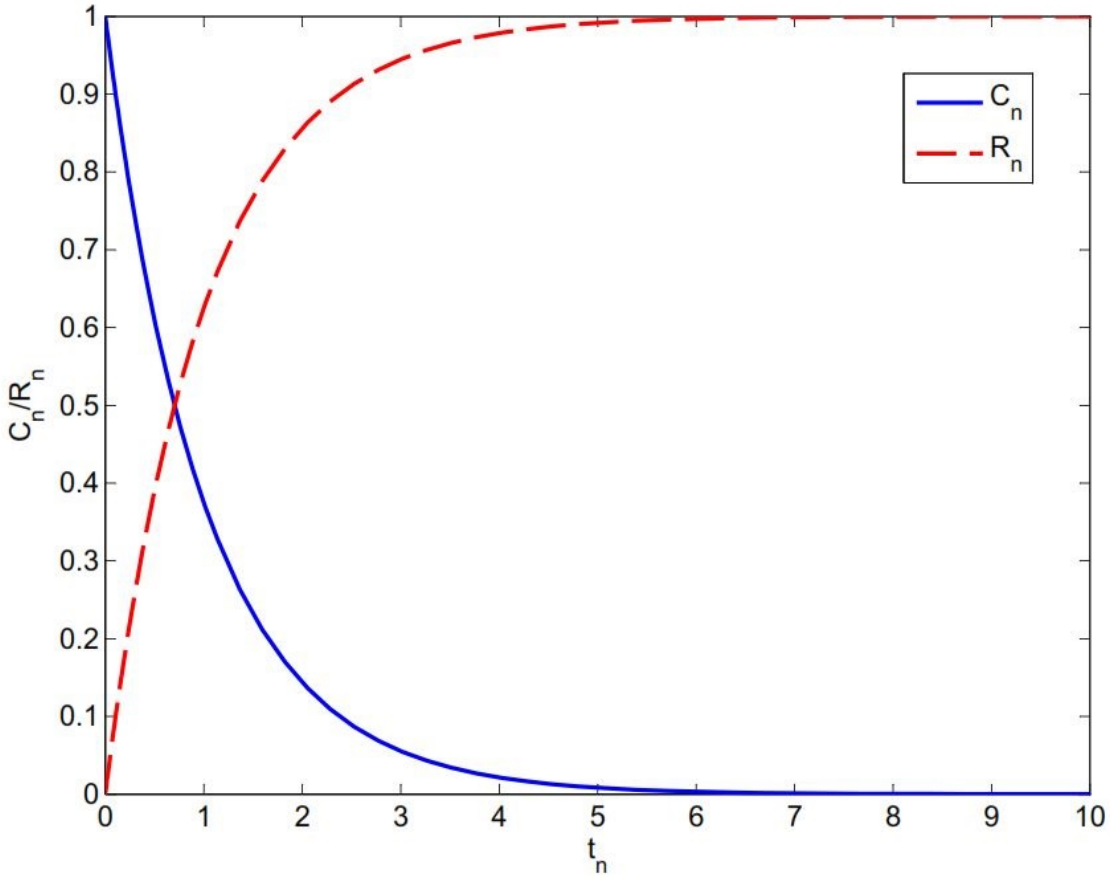

Figure 3.3. *Change of number of complexes and receptors on the cantilever surface with time*

In this model, two nondimensional parameters, A_n, and D_{Ln} have important effects on dissociation of ligands and diffusion from local layer. A_n determines the release rate of ligands from the cantilever surface. For special molecules with specific k_D, A_n has a limit based on surface coverage. When A_n is larger than D_{Ln}, we are in reaction control regime where the effect of unbinding of ligands from receptors on the cantilever surface and binding of ligands to receptors in the solution is dominant. In diffusion control regime, when D_{Ln} is much larger than A_n, ligand molecules tend to diffuse away from the local layer quickly and therefore, the diffusion effect is more dominant. We investigate the effects of these two parameters for different concentration of soluble receptors by considering three cases as follow:

Case 1: $A_n > D_{Ln}$

Case 2: $A_n = D_{Ln}$

Case 3: $A_n < D_{Ln}$

3.2.1. Case 1: $\boldsymbol{A_n > D_{Ln}}$

When A_n is about 2 and $D_{Ln}$is about 0.02, we are in reaction control regime. Figure 3.4 shows the effect of different initial concentrations on number of complexes on cantilever surface at this regime. As it can be seen from this plot, all the curves overlap each other at first time intervals when ligand molecules dissociate from the cantilever. After that, soluble receptor molecules penetrate the local layer and react with free ligands. Ligands are also diffuse from local layer to the bulk. When the concentration of receptors increases, these processes take place faster.

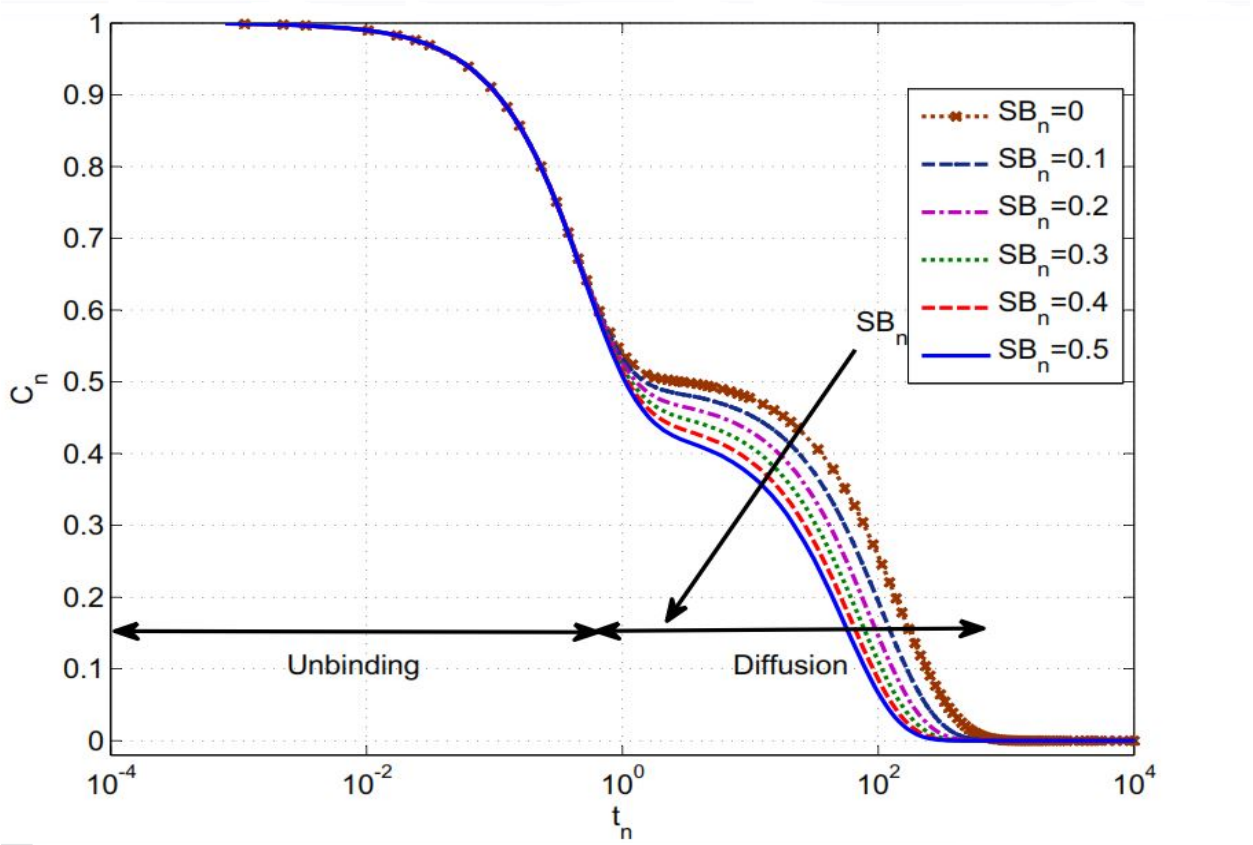

Figure 3.4. *Effect of soluble receptor concentration in reaction control regime*

3.2.2. Case 2: $A_n = D_{Ln}$

Figure 3.5 shows the effects of different initial concentrations on complex number when A_n and D_{Ln} are 2. Ligand molecules diffuse away from the local volume more quickly than in case 1 and the soluble receptor concentration has fewer effects on complexes number; therefore, detecting target molecule by competitive sensing method is difficult in this case.

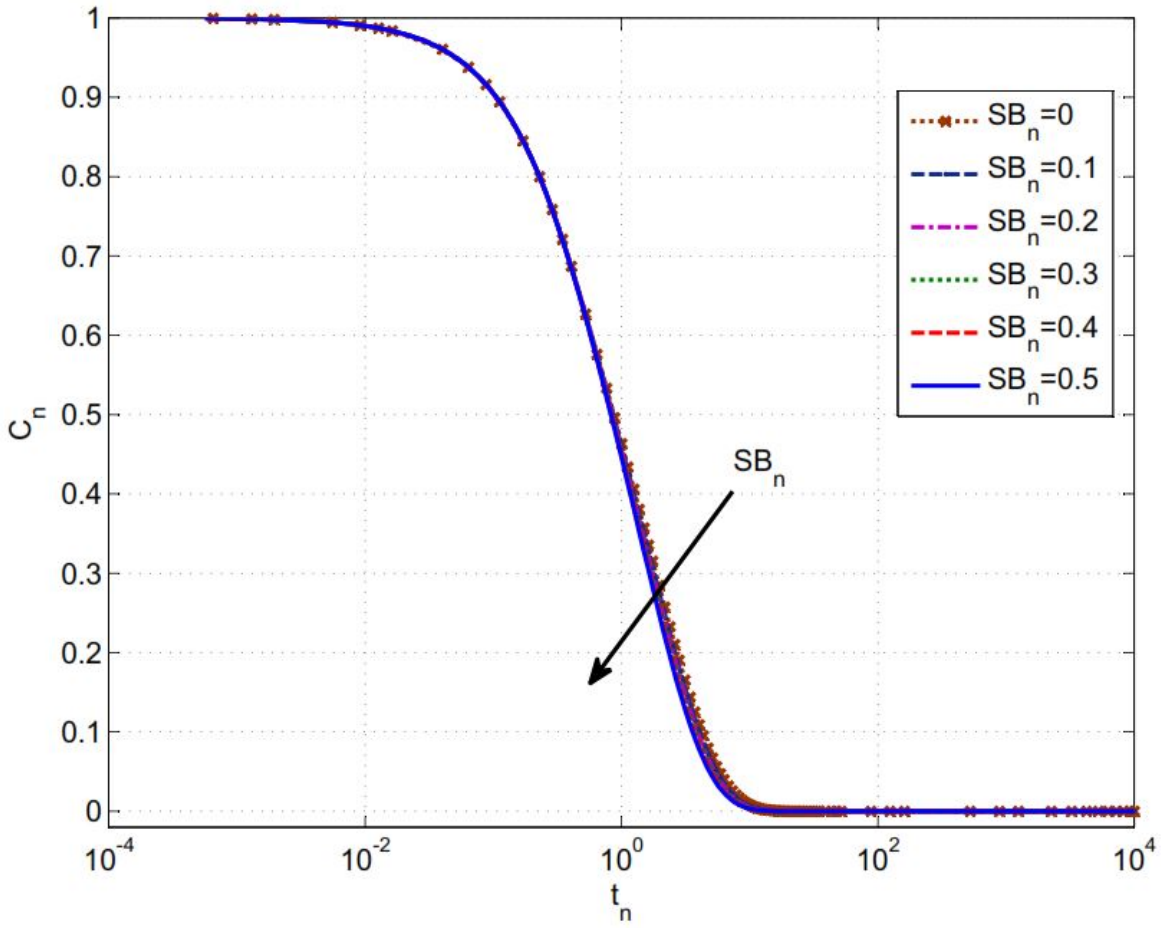

Figure 3.5. *Effect of soluble receptor concentration when A_n and D_{Ln} are equal*

3.2.3. Case 3: $A_n < D_{Ln}$

By comparing Figure 3.4 and 3.6, the difference in detecting target molecules in reaction control regime and diffusion control regime can be seen. In Figure 3.6, ligand molecules diffuse quickly from the local layer and interaction between these molecules and local soluble receptors less likely to happen in comparison with the situation when D_{Ln} was much smaller than A_n; therefore, the concentration of receptors in solution has almost no effects and detection of target molecules in this regime is almost impossible with this method.

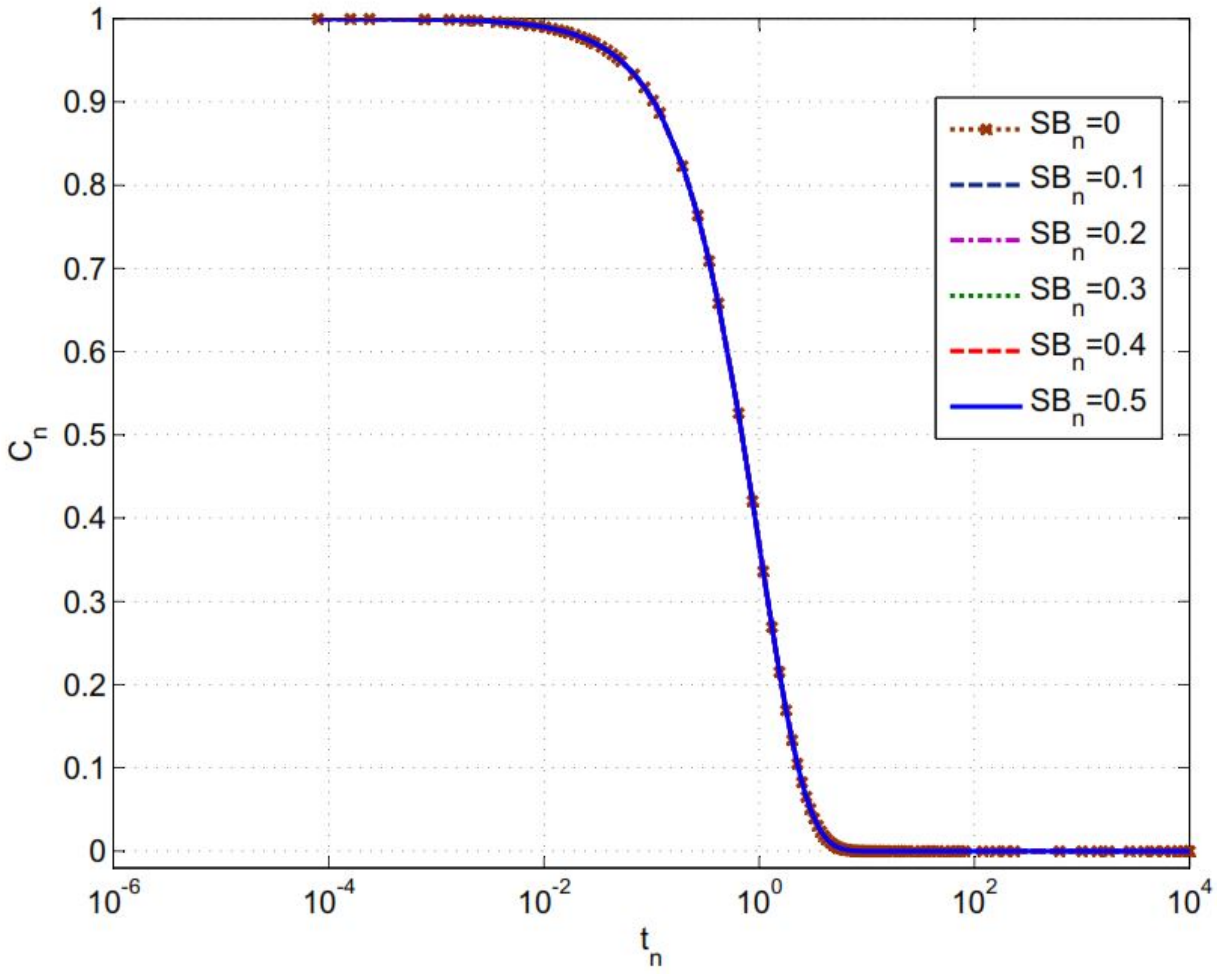

Figure 3.6. *Effect of soluble receptor concentration in diffusion control regime*

3.3. Effects of different parameters on reaction control regime

Figure 3.7 summarizes the effects of soluble receptor concentration in reaction control regime and diffusion control regime. Detection of target molecules in solution is easier when molecules are in reaction control regime and A_n is much larger than D_{Ln}.

Figure 3.8 shows the effect of different D_{Ln} on number of complexes when A_n is about 2 and SB_n is 0.5. For D_{Ln} of 20 and 200, we are in diffusion control regime and because in this regime, the model is less sensitive to reaction of molecules, it can be seen that the curves approximately overlap each other.

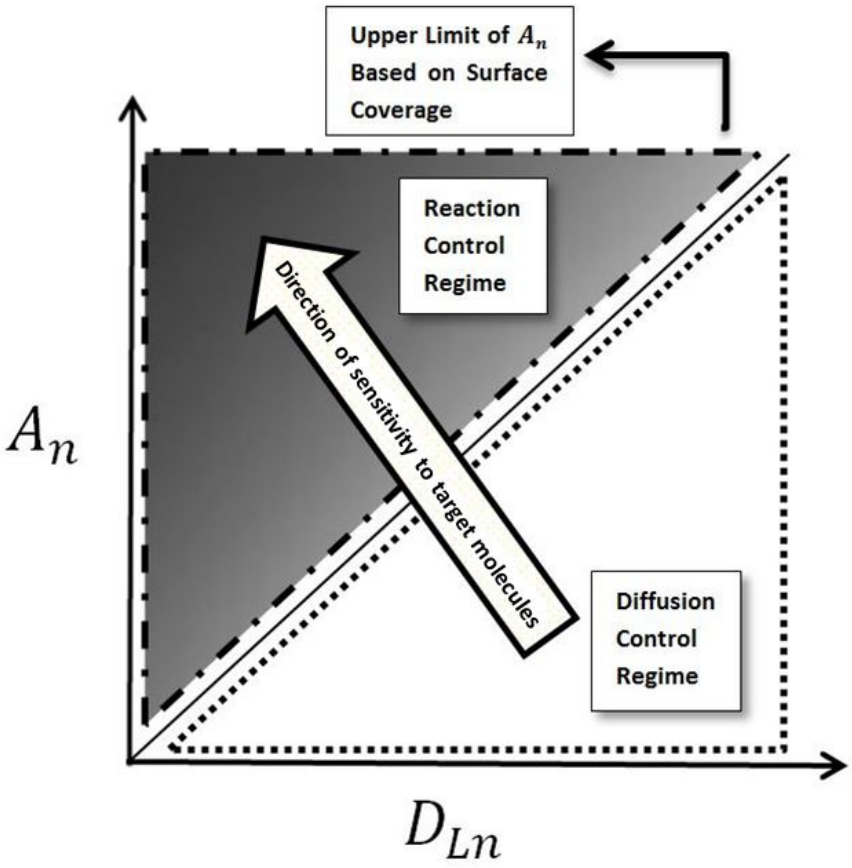

Figure 3.7. *Reaction control and Diffusion control regime*

Figure 3.9 shows the effects of different A_n on approximation of complex number rate for two different A_n where the complex number rate can be found from following equation:

$$\frac{\Delta C_n}{\Delta t_n} = \frac{C_n(t_{n2}) - C_n(t_{n1})}{t_{n2} - t_{n1}}. \tag{3.12}$$

Higher A_n is given for higher surface coverage and the curve trend for higher A_n can be compared with experimental results by Kang et al that have been shown in Figure 3.10 and prove that competition sensing mode works well in detection of target molecules in solution. This method is even able to detect different target molecules in the same solution

when the unbinding rates of the molecules in the solution are different. Assuming the same binding rate for different molecules, Figure 3.11 has been plotted for different k_fs when A_n is 20, D_{Ln} is 0.02, t_{n1} is 0.4 and t_{n2} is 0.8. The different complex number rate curves prove the ability of this method in sensing different target molecules.

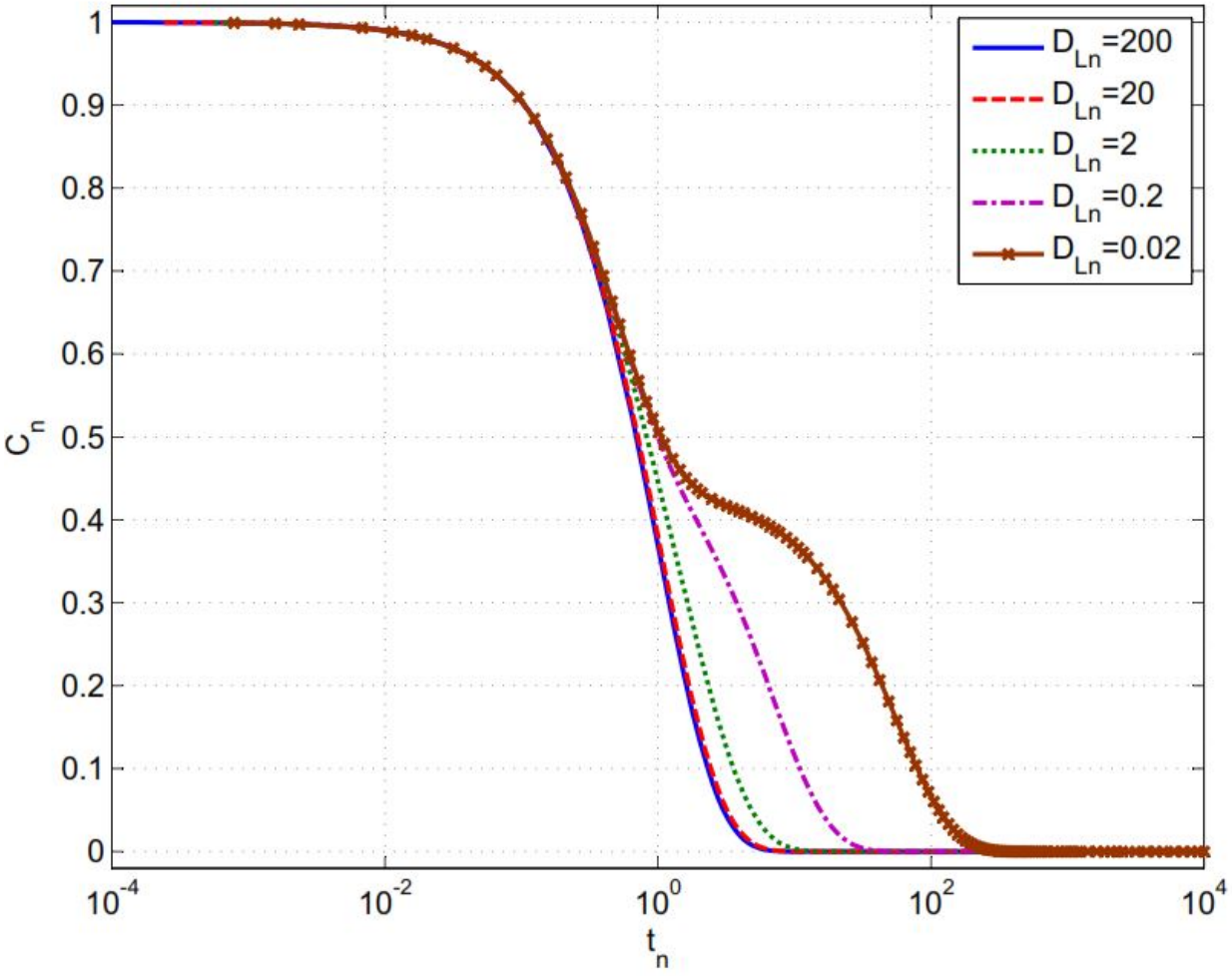

Figure 3.8. *Effect of different D_{Ln}on nondimensional complex number*

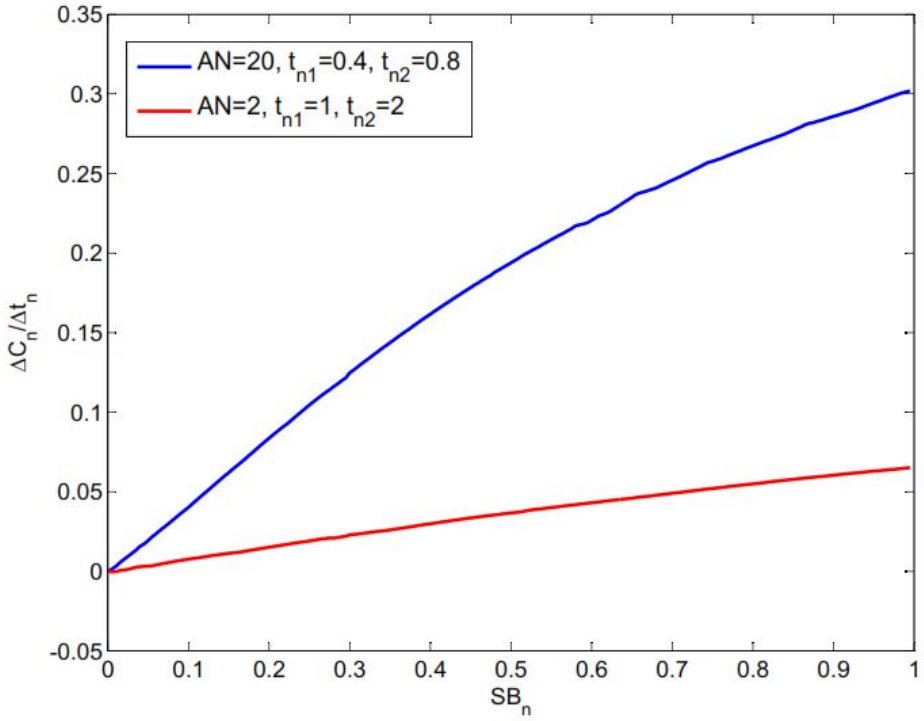

Figure 3.9. *Effect of different A_n on nondimensional complex number rate*

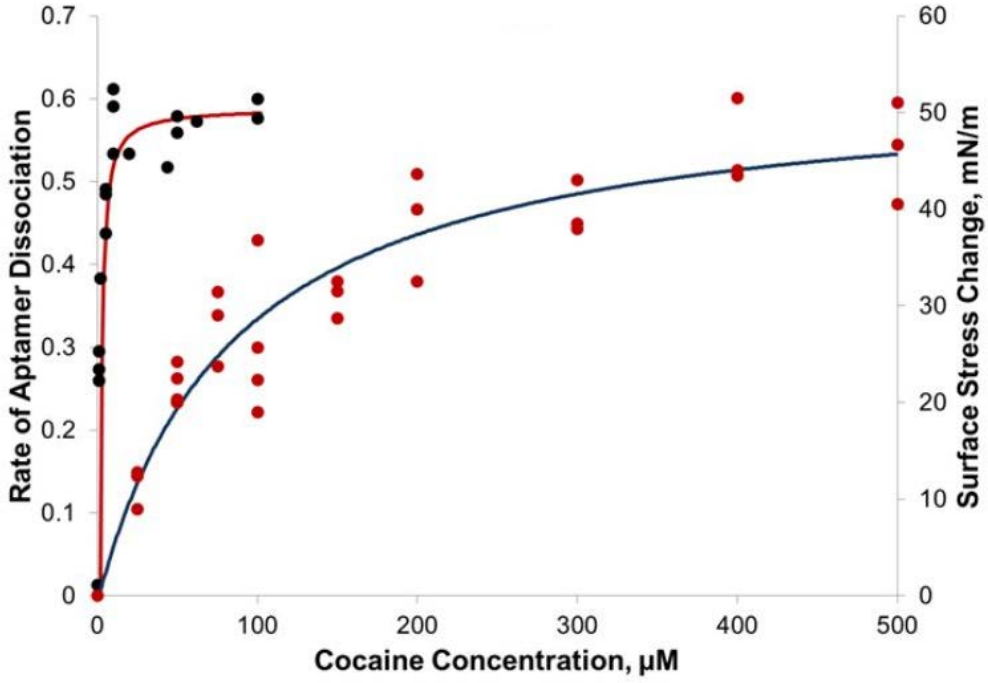

Figure 3.10 *Kang et al. [18] experimental results for conventional (red dots) and competition (black dots) sensing method*

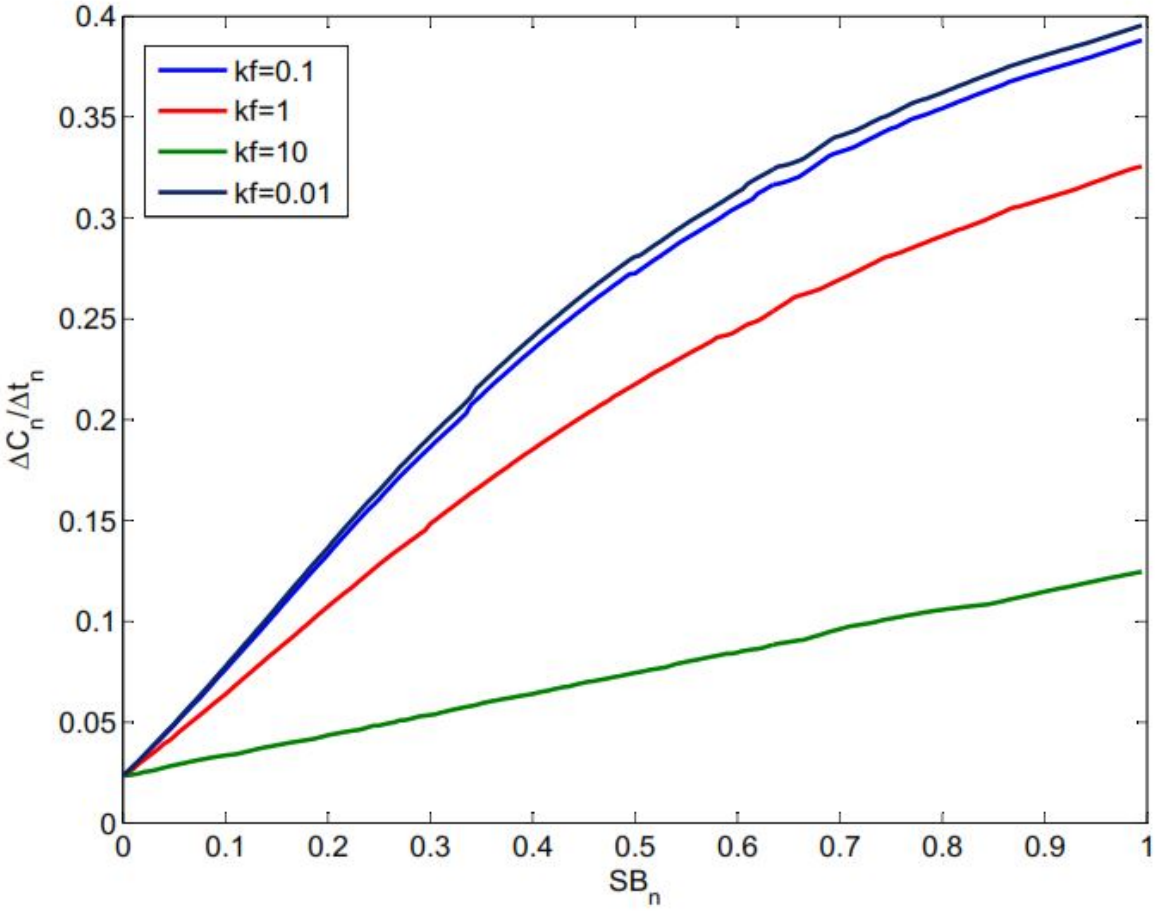

Figure 3.12. *Complex number rate against nondimensional soluble concentration for different* k_f

CHAPTER IV

SUMMARY AND CONCLUSION

4.1 Summary

Micro-cantilever biosensor can be used to detect target molecules in the solution with at least two different methods: conventional mode of sensing and competition mode of sensing. In conventional mode of sensing, interaction between molecules can cause cantilever deformation that shows the existence of target molecules in the solution. Electrostatic and hydrostatic forces as well as change in entropy of the system can have contribution in surface stress change in outer surface of the cantilever and consequently, cantilever tip deflection. In competition mode of sensing, the rate of cantilever deformation can shows the existence of target molecules. This method is useful when the concentration of target molecules in the solution is low and conventional method of sensing is unable to detect molecules.

4.2 Conclusions

In this report, two theoretical and mathematical models, molecular interaction model and entropy model for stand-up configuration of molecules were modified considering conventional mode of sensing and another model for lie-down configuration based on entropy change was proposed. The numerical results showed that the entropy model was unable to predict cantilever deflection when the molecular separation is much larger than molecule size; however, the molecular interaction model that is based on interaction between dsDNAs can give us reasonable results.

In addition, another model was developed for competition mode of sensing. It was shown that the competition sensing worked in reaction control regime when ligands molecules interacted with available receptors in the local layer before they diffused away from it. Also, sensing could be stronger when surface coverage of complexes were higher resulted in higher nondimensional number A_n. The trend of the curve for higher A_n was comparable with experimental results. The model also showed the competition sensing could be able to detect different target molecules with different unbinding rate constant in the same solution.

REFERENCES

[1] Lavrik, N.V., Sepaniak, M.J. and Datskos, P.G., 2004. “Cantilever transducers as a platform for chemical and biological sensors”. Rev. Sci. Instrum 75(7), 2229.

[2] Tamayo, J., Humphris, A.D.L, Malloy, A.M., and Miles, M.J., 2001. “Chemical sensors and biosensors in liquid environment based on microcantilevers with amplified quality factor”. Ultramicroscopy 86(1-2), 167-173.

[3] Wu, G., Datar, R.H., Hansen, K.M., Thundat, T., Cote, R.J. Majumdar, A., 2001, “Bioassay of prostate-specific antigen (PSA) using microcantilevers”. Nature. Biotechnol. 19(9) 856-860.

[4] Arntz, Y., Seelig, J.D., Lang, H.P., Zhang, J., Hunziker, P., Ramseyer, J.P., Meyer, E., Hegner, M. and Gerber, Ch., 2003. “Label-free protein assay based on a nanomechanical cantilever array”. Nanotechnology. 14(1), 86.

[5] Alvarez, M., Carrascosa, L.G., Moreno, M., Calle, A., Zaballos, A., Lechuga, L.M., Martinez, A.C., and Tamayo, J., 2004. “Nanomechanics of the formation of DNA self-assembled monolayers and hybridization on microcantilevers”. Langmuir. 20(22), 9663-9668.

[6] Jin, K.S., Shin, S.R. Ahn, B., Rho, Y., Kim, S.J., and Ree, M., 2009. “PH-dependent structures of an i-motif DNA in solution”. J. Phys. Chem. B. 113(7), 1852-1856.

[7] Kang, K., Nilsen-Hamilton, M., and Shrotriya, P., 2008. “Differential surface stress sensor for detection of chemical and biological species”. Appl. Phys. Lett. 93(14), 143107.

[8] Fritz, J., 2008. “Cantilever biosensors”. Analyst 133(7), 855-863.

[9] Fritz, J., Baller, M.K., Lang, H.P., Rothuizen, H., Vettiger, P., Meyer, E., Guntherodt, H.-J., Garber, Ch., and Gimzewski, J.K., 2000. “Translating bimolecular recognition into nanomechanics”. Science. 288(5464), 316-318.

[10] Hansen, K.M., Ji, H.F., Wu, G., Datar, R., Cote, R. Majumdar, A., and Thundat, T., 2001. “Cantilever-based optical deflection assay for discrimination of DNA single-nucleotide mismatches”. Anal. Chem. 73(7), 1567-1571.

[11] Stachowiak, J.C., Yue, M., Castelino, K., Chakraborty, A., and Majumdar, A., 2006. “Chemomechanics of surface stresses induced by DNA hybridization”. Langmuir. 22(1), 263-268.

[12] Hagan, M.F., Majumdar, A. and Chakraborty, A.K., 2002. “Nanomechanical forces generated by surface grafted DNA”. J. Phys. Chem. B. 106(39), 10163-10173.

[13] Begley, M.R., Utz, M., Komaragiri, U., 2005. “Chemo-mechanical interaction between adsorbed molecules and thin elastic films”. J. Mech. Phys. Solids. 53(9), 2119-2140.

[14] Huang, L., Seker, E., Landers, J.P., Begley, M.R., and Utz, M., 2010. “Molecular Interaction in surface-assembled monolayers of short double-stranded DNA”. Langmuir. 26(13), 11574-11580.

[15] Strey, H.H., Parsegian, V.A., and Podgornik, R., 1997. “Equation of state for DNA liquid crystals: fluctuation enhanced electrostatic double layer repulsion”. Phys. Rev. Lett. 78(5), 895-898.

[16] Strey, H.H., Parsegian, V.A., and Podgornik, R., 1999. “Equation of state for polymer liquid crystals: Theory and experiment”. Phys. Rev. E. 59(1), 999-1008.

[17] Zhao, Y., Ganapathysubramanian, B., Shrotriya, P., 2012. “Cantilever deflection associated with hybridization of monomolecular DNA film”. J. Appl. Phys. 111(7), 074310.

[18] Kang, Kyungho, "MicroCantilever (MC) based nanomechanical sensor for detection of molecular interactions" (2011). *Graduate Theses and Dissertations.* Paper 12148.

[19] Allen, M.P., and Tildesley, D.J., 1987. “Statistical Mechanics.” Computer Simulation of Liquids. 1st ed. New York: Oxford UP, 46-50.

[20] Forsten, K.E., Lauffenburger, D.A., 1992. “ Autocrine ligand binding to cell receptors. Mathematical analysis of competition by solution "decoys"”. Biophys. J. 61(2), 518-529.

[21] Forsten, K.E., Lauffenburger, D.A., 1992. “Interrupting autocrine ligand-receptor binding: comparison between receptor blockers and ligand decoys”. Biophys. J. 63(3), 857-861.

[22] Smoluchowski, M.V., 1916. “Versuch einer mathematischen Theorie der Koagulationskinetic kolloider Lösungen”. Z. Phys. Chem. 92, 129–168.

[23] Peters, M.H., 2000. “The Smoluchowski diffusion equation for structured macromolecules near structured surfaces”. 112(12), 5488-5498.

[24] Bao, J., Krylova, M., Reinstein, O., Johnson, P.E., and Krylov, S.N., 2011. “Label-free solution-based kinetic study of aptamer_small molecule interactions by kinetic capillary electrophoresis with UV detection revealing how kinetics control equilibrium”. Anal. Chem. 83(22), 8387-8390.